NASA Contractor Report 198513

Active Control of Fan Noise: Feasibility Study

Volume 5: Numerical Computation of Acoustic Mode Reflection Coefficients for an Unflanged Cylindrical Duct

R.E. Kraft
General Electric Aircraft Engines
Cincinnati, Ohio

September 1996

Prepared for
Lewis Research Center
Under Contract NAS3–26617

National Aeronautics and
Space Administration

Active Control of Fan Noise: Feasibility Study
Volume 5: Numerical Computation of Acoustic Mode Reflection Coefficients for an Unflanged Cylindrical Duct

Summary

A computational method to predict modal reflection coefficients in cylindrical ducts has been developed based on the work of Lordi, Homicz, and Rehm, which uses the Wiener-Hopf method to account for the boundary conditions at the termination of a thin cylindrical pipe. The purpose of this study is to develop a computational routine to predict the reflection coefficients of higher order acoustic modes impinging on the unflanged termination of a cylindrical duct.

This effort was conducted under Task Order 5 of the NASA Lewis LET Program, *Active Noise Control of Aircraft Engines: Feasibility Study*, and will be used as part of the development of an integrated source noise, acoustic propagation, ANC actuator coupling, and control system algorithm simulation.

The reflection coefficient prediction will be incorporated into an existing cylindrical duct modal analysis to account for the reflection of modes from the duct termination. This will provide a more accurate, rapid computation design tool for evaluating the effect of reflected waves on active noise control systems mounted in the duct, as well as providing a tool for the design of acoustic treatment in inlet ducts. As an active noise control system design tool, the method can be used preliminary to more accurate but more numerically intensive acoustic propagation models such as finite element methods.

The resulting computer program has been shown to give reasonable results, some examples of which are presented. Reliable data to use for comparison is scarce, so complete checkout is difficult, and further checkout is needed over a wider range of system parameters. In future efforts the method will be adapted to provide input reflection coefficients to the GEAE segmented cylindrical duct modal analysis prediction program.

Active Control of Fan Noise: Feasibility Study
Volume 5: Numerical Computation of Acoustic Mode Reflection Coefficients for an Unflanged Cylindrical Duct

Table of Contents

Active Control of Fan Noise: Feasibility Study
Volume 5: Numerical Computation of Acoustic Mode Reflection Coefficients for an Unflanged Cylindrical Duct

1. Introduction

1.1 Study Assumptions and Objectives

The purpose of this study was to develop a computational routine to predict the reflection coefficients of higher order acoustic modes impinging on the unflanged termination of a cylindrical duct. This prediction will be incorporated into the existing cylindrical duct modal analysis to account for the reflection of modes from the duct termination. This will provide a more accurate, rapid computation design tool for evaluating the effect of reflected waves on active noise control (ANC) systems mounted in the duct[1], as well as providing a tool for the design of acoustic treatment in inlet ducts. As a treatment design tool, the method can be used preliminary to more accurate but more numerically intensive acoustic propagation models such as finite element methods.

The classical duct modal analysis[2] provides an exact solution to duct propagation in treated ducts, accurate to the convergence afforded by the number of modes used in the solution expansion. It is limited in the sense of requiring idealized geometry; the duct must be cylindrical with constant radius along its axis, and the reflection coefficient is that for a cylindrical pipe with infinitely thin walls. Aircraft engine ducts have variable duct radius and nacelles with finite thickness and rounded ends.

The cylindrical duct modal analysis does allow axial discontinuities in acoustic treatment properties (segmented treatment), but allows no circumferential nonuniformities. It calculates one frequency and one spinning mode order at a time, assuming coupling among the radial modes but no coupling among spinning modes.

The modal analysis should be sufficiently accurate to allow evaluation of active noise control concepts when adapted as part of a simulation model that includes the coupling of the ANC actuators to the duct walls and the ANC feedback control system. If required, more accurate prediction and confirmation of ANC or treatment suppression or farfield radiation absolute levels can subsequently be done with a more accurate prediction model (such as FEM).

An objective was to develop a reflection coefficient computational routine that is reasonably rapid when coupled to the modal analysis, so that treatment design parametric studies involving many cases with different frequencies and spinning mode orders are practical and efficient. If only the treatment parameters change, the reflection coefficients can be stored and re-used, increasing efficiency for multiple case runs. Twenty years ago, when the segmented duct modal analyses were first developed, such a reflection

coefficient routine was developed and incorporated into a segmented duct modal analysis[3], but it took so long to compute the coefficients that it was seldom used.

1.2 The Weiner-Hopf Technique

The approach in this study is founded upon the prior work of Lordi, Homicz, and Rehm[4], (LHR) particularly as detailed in the second volume of their Air Force contract final report[5]. This work is based on the Wiener-Hopf solution for the reflection and radiation of waves propagating in a pipe, and it, in turn, is based on the prior work of several researchers[6,7,8].

The Wiener-Hopf technique[9] is a very complicated mathematical method for solving boundary value problems involving semi-infinite waveguides that radiate to the farfield. The method transforms the partial differential wave equation and the semi-infinite waveguide boundary conditions using spatial Fourier transforms (in wavenumber space) to convert the solution to integral equation form. Solution of the integral equation requires a special factorization of the kernel, invocation of properties of complex analytic functions, and subsequent inversion of the Fourier transform in complex space using contour integrals.

The method, although straightforward in principle, is not unique in the form of separating the kernel, and requires application of advanced methods of complex variable integral calculus to arrive at a solution that is, more or less, computable. Part of the solution manifests itself in closed form, and part of the solution still requires a numerical integration. The many steps in the derivation and the invocation of esoteric theorems of complex analysis, as well as dealing with Bessel functions and their identities, make the entire procedure very error-prone.

The effort in this development makes no claims of being particularly original. The application of the Wiener-Hopf method by Lordi, Homicz, and Rehm to the case of higher order spinning modes in a cylindrical pipe was assumed to be derived correctly, and, up to the point where they begin to put results in computational form, the derivation was not checked step-by-step. LHR present final equations that are almost, but not quite, ready for computation. This analysis picks up at a particular stage of the LHR derivation and develops a computation that gives reasonable results and runs quickly on an IBM-PC. Final debugging and checkout of the computer program is still in progress. Unfortunately, reliable data against which to check the computation is scarce.

1.3 Modal Solution in a Cylindrical Duct

To define the modal reflection coefficients for wave propagation in a cylindrical duct, we present the form of the modal acoustic pressure as given by LHR for the m^{th} radial mode of the n^{th} order spinning mode:

$$p_{nm}(r,z,t) = A_{nm}\left[e^{ik_{nm}z}J_n\left(\gamma_{nm}\frac{r}{a}\right) + \sum_{j=1}^{\infty} R_{nmj}e^{-ik_{nj}z}J_n\left(\gamma_{nj}\frac{r}{a}\right)\right]e^{-i\omega t} \qquad (1\text{-}1)$$

where

r = duct radius

z = axial variable

t = time

n = spinning mode order ($-\infty < n < \infty$)

m = radial mode number (starting from m = 1 to ∞)

p_{nm} = (n,m) pressure mode

A_{nm} = (n,m) pressure mode coefficient

k_{nm} = (n,m) mode axial propagation constant (axial wavenumber)

$J_n(x)$ = n^{th} order Bessel function of first kind

γ_{nm} = (n,m) hardwall cylindrical duct eigenvalue

a = duct radius

R_{nmj} = reflection coefficient for reflection of radial mode m into radial mode j

ω = circular frequency ($2\pi f$)

The complete n^{th} order spinning mode solution for the pressure in the duct is the superposition of all pressure modes over index m. The cylindrical (inlet) duct geometry is shown in Figure 1.

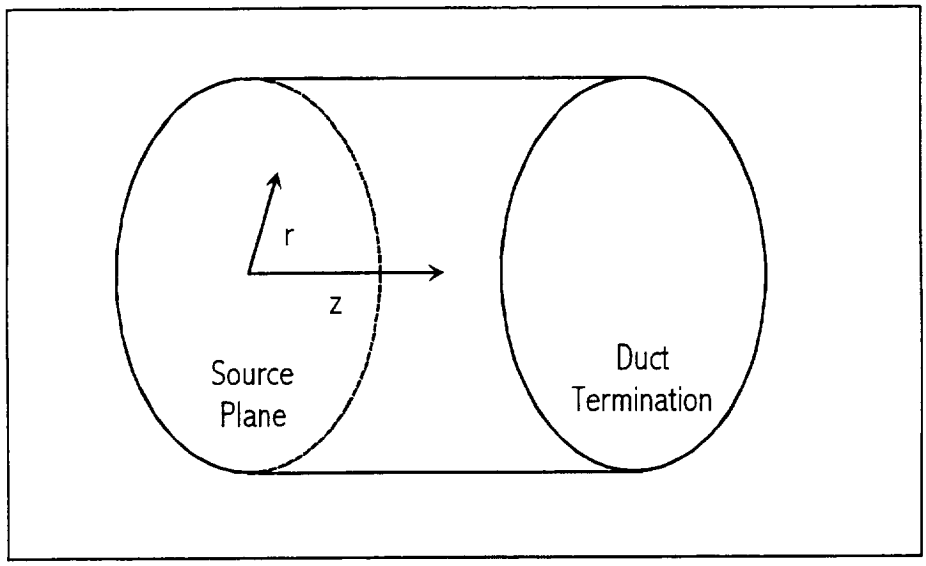

Figure 1 Duct geometry and coordinate system.

Note that the sum over modes involving the reflection coefficient, index j, goes to infinity, which implies that all cut-off modes must be included in this summation. A basic assumption of this study will be that the reflection coefficient sum can be approximated by summing only to the highest cut-on mode order, denoted by m_0, so that reflections into cut-off modes are neglected (in effect, cut-off mode reflection coefficients are set to zero).

This will not cause an error in the cut-on mode reflection coefficient calculation, and it may be assumed that energy reflected into cut-off modes will attenuate very quickly. The reflected cut-off modes may have an effect on the overall segmented duct solution for ducts with very short segments at the termination end. Including the computation of cut-off mode reflection coefficients should be considered for future program upgrades.

2. Basic Equations for the Reflection Coefficient

Given the spinning mode order, n, the reflection coefficient for the reflection of the m^{th} radial mode into the j^{th} radial mode at the termination of an unflanged circular duct, based on the LHR analysis, is

$$R_{nmj} = \frac{i\gamma_{nj}^2}{2k_{nj}a} \frac{\sqrt{(ka + k_{nm}a)(ka + k_{nj}a)}\, K_+(k_{nm}a) K_+(k_{nj}a)}{(k_{nm}a + k_{nj}a)(n^2 - \gamma_{nlj}^2)} \frac{J_n(\gamma_{nm}^2)}{J_n(\gamma_{nj}^2)} \tag{2-1}$$

where

n = spinning mode order
m,j = radial mode indices
γ_{nm} = (n,m) mode eigenvalue
k_{nm} = (n,m) mode axial propagation constant
a = duct radius
$k = \omega/c$
c = speed of sound

The axial propagation constant k_{nm} is given by

$$k_{nm}a = \sqrt{(ka)^2 - \gamma_{nm}^2} \tag{2-2}$$

and the mode eigenvalues γ_{nm} are determined as the roots of the equation

$$J_n'(\gamma_{nm}) = 0 \tag{2-3}$$

These are the eigenvalues for the modes in a hardwall circular duct, determined from the boundary condition that requires the normal acoustic velocity (or derivative of pressure) to be zero at the wall.

The K_+ are defined as functions of argument ζa by

$$K_+(\zeta a) = \sqrt{\pi(ka - \zeta a)}\, J_n'(v)\, H_n^{(1)\prime}(v)}\; e^{\frac{1}{2}M(\zeta a)} \tag{2-4}$$

for $n > 0$, where $H_n^{(1)}$ is the Hankel function of the first kind, and

$$v = v(\zeta a) = \sqrt{(ka)^2 - (\zeta a)^2} \tag{2-5}$$

From references on Bessel functions, we can write the Bessel function derivatives and the definition of the Hankel function derivative as

$$J'_n(v) = \frac{n}{v} J_n(v) - J_{n+1}(v) \tag{2-6}$$

$$H'^{(1)}_n(v) = J'_n(v) + iY'_n(v) \tag{2-7}$$

$$Y'_n(v) = \frac{n}{v} Y_n(v) - Y_{n+1}(v) \tag{2-8}$$

The function $M(\zeta a)$ in Equation (2-4) is given by the integral

$$M(\zeta a) = \frac{2\zeta a}{\pi} \sum_{m=1}^{\infty} \left[\int_{k_{n,m-1}a}^{k_{n,m}a} \frac{\Omega(v) - \Omega(v_{n,m-1})}{(\zeta a)^2 - (wa)^2} d(wa) \right] \tag{2-9}$$

where

$$k_{n0}a = ka \tag{2-10}$$

otherwise k_{mn} is defined by Equation (2-2). The function $M(\zeta a)$ is a contour integration shown by LHR[10] to arise from the Wiener-Hopf kernel factorization procedure.

The function $\Omega(v)$ is defined by

$$\Omega(v) = \arctan\left[\frac{Y'_n(v)}{J'_n(v)}\right] - \frac{\pi}{2} \qquad (n > 0) \tag{2-11}$$

where

$$\Omega(0) = 0 \tag{2-12}$$

$$v_{nm} = \sqrt{(ka)^2 - (k_{nm}a)^2} \tag{2-13}$$

$$\Omega(v_{nm}) = (m-1)\pi \tag{2-14}$$

Equation (2-14) defines the branch of the arctangent function to be chosen for each mode, and guarantees that $\Omega(v)$ is continuous as the arctangent goes through each cycle of π. Use of Equation (2-14) necessitates keeping track of the arctangent branch when passing from one modal segment to the next in Equation (2-9).

The path of the M-integral in Equation (2-9) is shown in Figure 2. The path proceeds backwards along the real axis starting at wa = ka and includes all cut-on modes before it reaches wa = 0. The index m_0 denotes the highest order cut-on mode. The integral proceeds along the real axis to zero, then heads up the imaginary axis, where it picks up all cut-off modes. The parameter ζa is a pole on the real axis (for the reflection coefficient calculation $\zeta a = k_{nm}a$). The integration to high cut-off mode orders should eventually converge, since the denominator of the M-integral goes to infinity as i·wa goes to infinity.

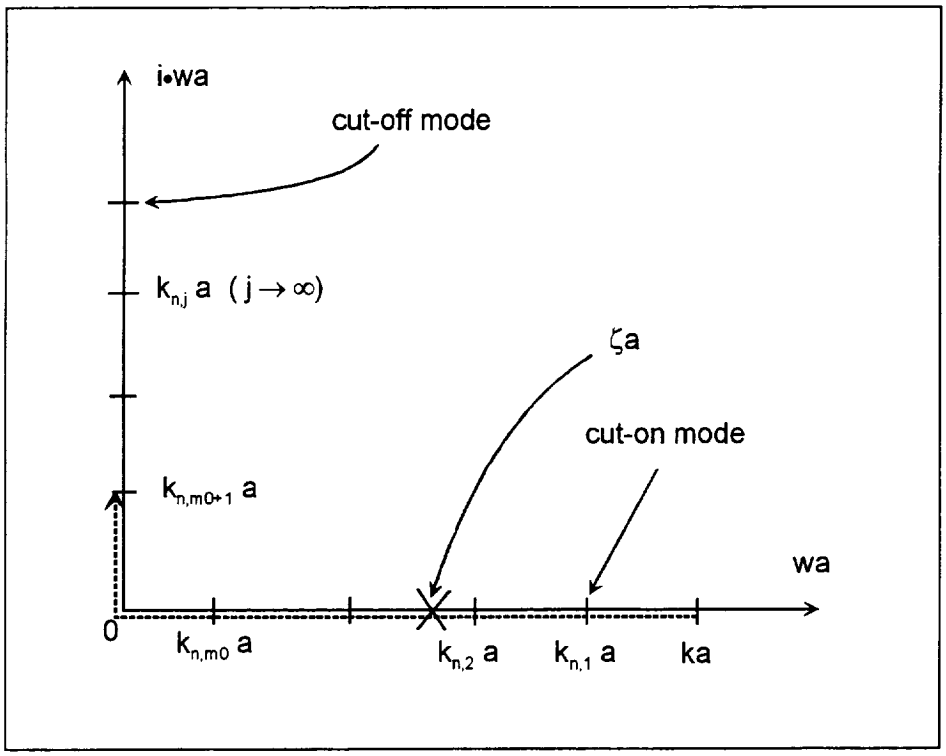

Figure 2. M-integral integration path in complex plane (dashed line)

The parameter ζa takes on different meanings depending upon whether the reflection coefficient or the farfield radiation is being calculated. For the reflection coefficient calculation, ζa takes on only the values $k_{nm}a$, for all modes m. Thus, it is located only at intersections between modal integration segments on the real axis, and the poles involve the endpoints of two adjacent integration segments. For the farfield radiation calculation, the ζa may occur inside any segment, as well as at the endpoints.

3. Behavior of the Integrand of the M-Integral

The function $M(\zeta a)$, defined in Equation (2-9), has a direct effect on the value of reflection coefficient R_{nmj} through the K_+ factor, defined in Equation (2-4). The computation of the integral in $M(\zeta a)$, which we shall refer to as the M-integral, is the most difficult aspect of the entire reflection coefficient calculation. The M-integral can be split into two terms:

$$GV = \frac{2\zeta a}{\pi} \sum_{m=1}^{\infty} \int_{k_{n,m-1}a}^{k_{nm}a} \frac{\Omega(v)}{(\zeta a)^2 - (wa)^2} d(wa) \tag{3-1}$$

and

$$GC = -\frac{2\zeta a}{\pi} \sum_{m=1}^{\infty} \int_{k_{n,m-1}a}^{k_{nm}a} \frac{\Omega(v_{n,m-1})}{(\zeta a)^2 - (wa)^2} d(wa) \tag{3-2}$$

where GV is referred to as the variable-Ω part of the M-integral and GC as the constant-Ω part. Both integrals are written as a sum over all cut-on and cut-off modes.

It is instructive to examine the behavior of the integrand functions of the M-integral, particularly the function $\Omega(v)$, over the real axis from ka down to zero. As a sample case, we shall use the following set of parameters:

Spinning mode order, n = 2
ka = 12.5

For these conditions, there are three cut-on modes that have the eigenvalues and propagation constants given in Table 1.:

Radial mode order m	Eigenvalue γ_{2m}	Axial wavenumber k_{2m}
1	3.054237	12.12112
2	6.706133	10.54883
3	9.969468	7.540437

Table 1. Test case mode eigenvalues and propagation constants

We are examining in particular the variable-Ω part of the M-integral over the real axis for $0 \le wa \le ka$. The integrand for this integral may be written as

$$\frac{\Omega(v)}{\zeta a^2 - wa^2} = \frac{\Omega(v)}{(\zeta a - wa)(\zeta a + wa)} = \frac{Q(v)}{\zeta a - w} \tag{3-3}$$

where Q(v) is the non-singular factor in the integrand,

$$Q(v) = \frac{\Omega(v)}{\zeta a + wa} \tag{3-4}$$

We shall examine $\Omega(v)$, Q(v), and the complete integrand separately, with ζa chosen arbitrarily as the second mode wavenumber, $\zeta a = 10.54883$.

The MathCAD program FCM2.MCD, used to carry out the above computations, was used to generate the output in Figure 3, and shows what values are obtained when the Ω-function is calculated directly from the arctangent function definition, using simply the arctangent principle value. Notice that as the Bessel function derivatives wind through their zero-values, the arctangent has discontinuities when the principle value cycles through π. The function can be made continuous by adding an appropriate multiple of π, depending on how many cycles have been accumulated.

When Ω is re-defined to include these branch cut shifts, the function becomes continuous, as illustrated in the FORTRAN-generated plot shown in Figure 4. Notice here that the Ω-function is continuous at the intersections between mode segments, and that the wa-axis is plotted backwards, in the direction of integration.

Figure 5. shows the non-singular part of the integrand, Q(v), for this case. This function is well-behaved within the real axis integration limits, as long as $\Omega(v)$ is properly defined.

Finally, note the behavior of the full integrand in Figure 6., with a first-order pole at $\zeta a = 10.54883$. A special Cauchy principle value integration procedure must be used to compute this improper integral containing a singularity.

The constant-Ω part of the M-integral differs in that Ω undergoes a discontinuous jump in otherwise constant value as the junction of endpoints between two modal segments is crossed by the integration. The integrals, however, can be computed in closed form within each modal segment, with special attention to the integration across the pole.

The integrands for the part of the M-integral up the imaginary axis pose no additional special problems, and will be considered later. By limiting ζa to real values, we are limiting the reflection coefficients to include only cut-on modes. This allows the effects of cut-off modes to be included in the computation of each cut-on mode reflection coefficient, but omits the reflection coefficients for cut-off modes themselves. This avoids the (not too difficult) problem of complex values of ζa, which would lead to poles along the imaginary axis. Other than causing programming difficulties with the complex algebra, there is no practical reason why cut-off modes could not be included, but this will be left for future program upgrades.

$$FJ(m,x) := \frac{m}{x} \cdot Jn(m,x) - Jn(m+1,x) \qquad m := 2$$

$$FY(m,x) := \frac{m}{x} \cdot Yn(m,x) - Yn(m+1,x) \qquad ka := 12.5$$

$$w := 0.,.01.. 12.45$$

$$\Omega(m,x) := \operatorname{atan}\left(\frac{FY(m,x)}{FJ(m,x)}\right) - \frac{\pi}{2} \qquad x(w) := \sqrt{ka^2 - w^2}$$

Bessel Functions

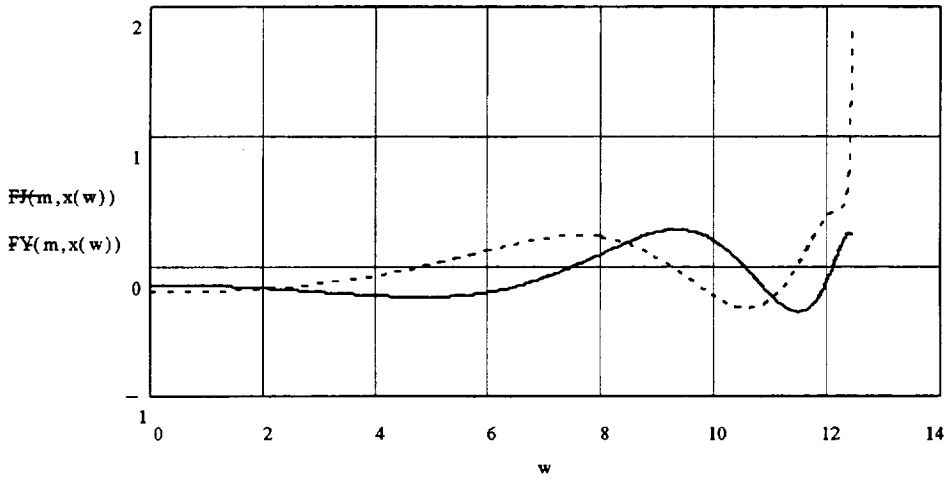

Function Ω

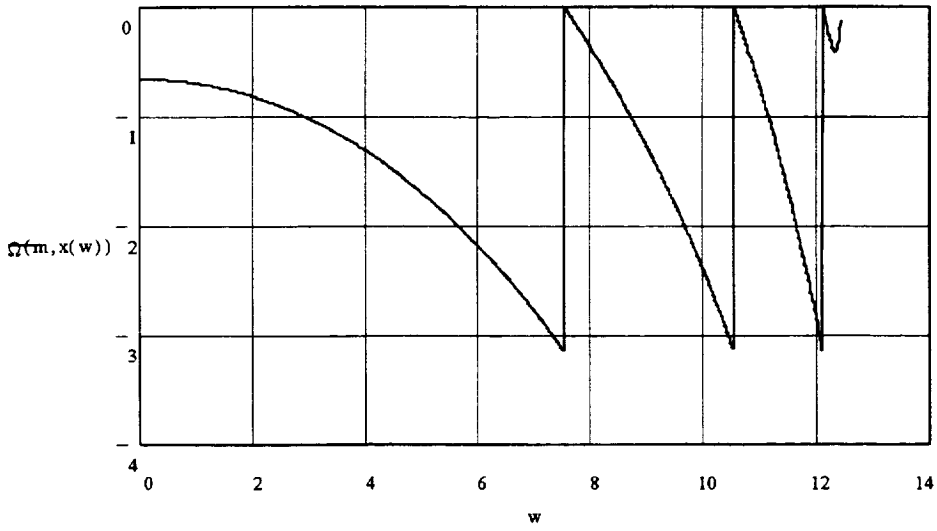

Figure 3. Behavior of functions in Homicz and Lordi integral

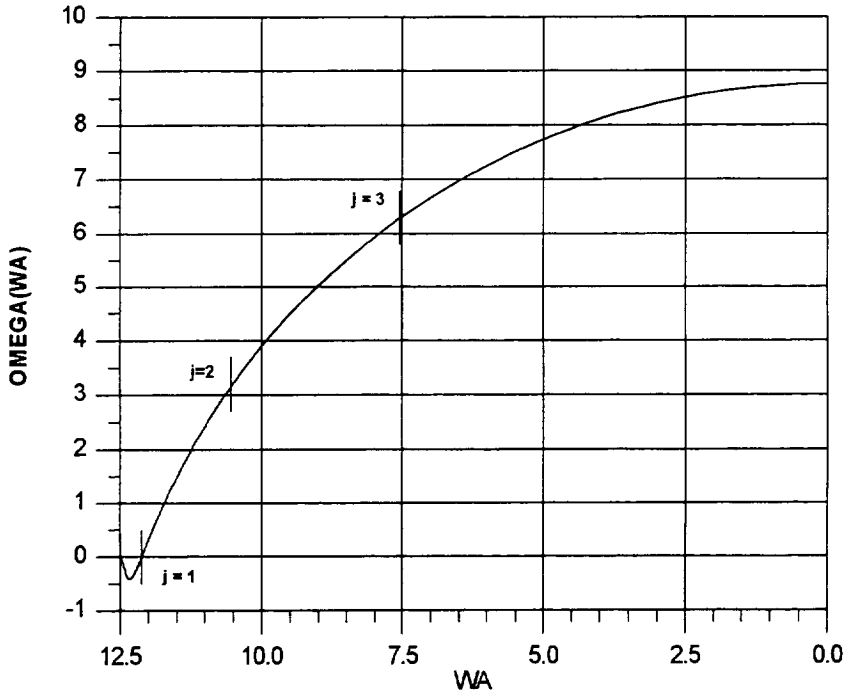

Figure 4. Function Ω for m = 2, ka = 12.5

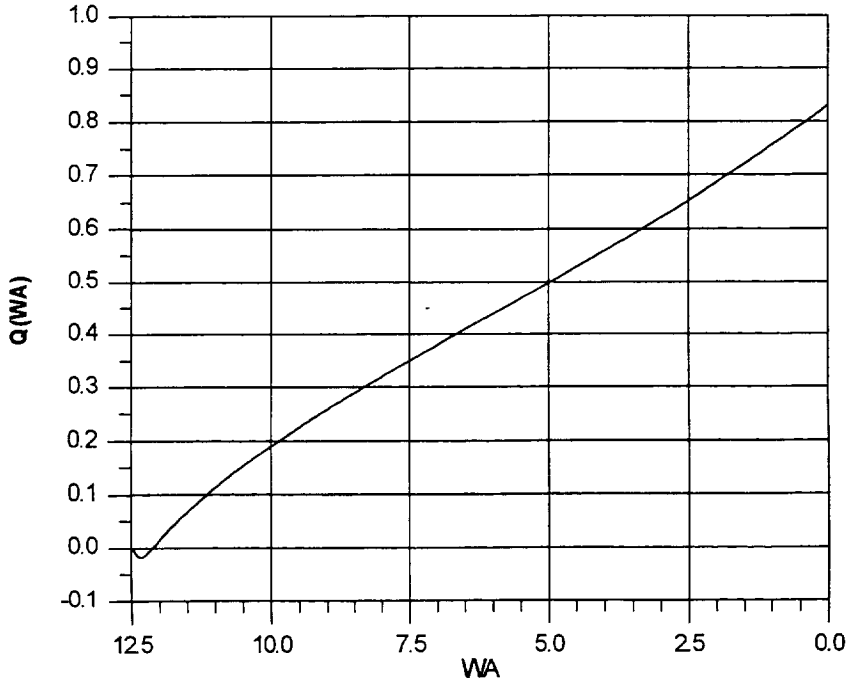

Figure 5. Function Q(wa) for m = 2, ka = 12.5, ξa = 10.54883

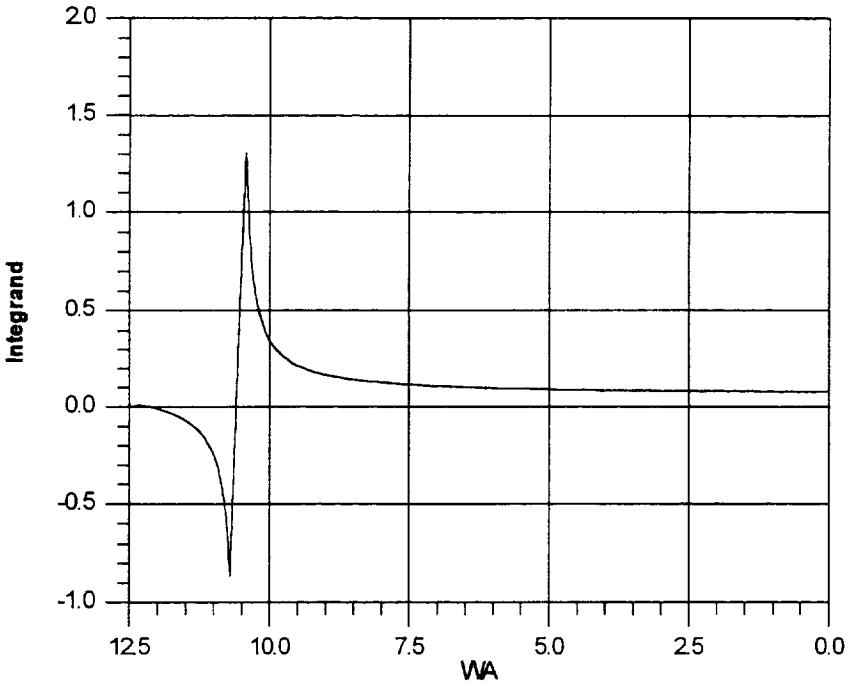

Figure 6. M-Integral integrand for m = 2, ka = 12.5, showing pole at $\zeta a = 10.54883$.

4. Computation of the M-Integral

4.1 Real Axis, Variable Ω

This integral, for each modal segment, can be written

$$GMVR(m) = \int_{k_{n,m-1}a}^{k_{nm}a} \frac{\Omega(v)}{(\zeta a)^2 - (wa)^2} d(wa) \tag{4-1}$$

where

$$k_{n0}a = ka \tag{4-2}$$

and m goes from m = 1 to m = m_0, where m_0 is the highest order cut-on mode. In addition, there is the partial segment

$$GMVR(m_0 + 1) = \int_{k_{n,m0}a}^{0} \frac{\Omega(v)}{(\zeta a)^2 - (wa)^2} d(wa) \tag{4-3}$$

which completes the full real axis range of $0 \le wa \le ka$.

Over a "clean" segment that contains no poles at either endpoint, this integral must be computed numerically. A Romberg FORTRAN integration subroutine[11] has been adopted for this purpose, and it converges rapidly for clean segments.

The part of the integration that requires special care is the choice of the correct branch of Ω(v) for the segment. The segment endpoints are obtained from the roots of the derivatives of the Bessel function of the first kind (Equation (2-3)). A subroutine to compute these roots is provided with the program.

This Bessel function root extraction program is accurate to about 1E-6 in single-precision arithmetic, so that when Ω(v) is computed close to an endpoint in the numerical integration scheme, care must be taken not to slip to the other side of the root, which will cause a discontinuity in Ω(v) and the integrand. To ensure that a particular numerical integration remains entirely within the proper segment, so that Ω(v) is computed with the correct multiple of π adder, the limits of integration are started and stopped arbitrarily 0.001 units of wa from the endpoints of the segment.

This causes a small error in the computation, but avoids a much larger error that would result from the Romberg scheme with a discontinuous integrand, not to mention an extreme time penalty as the Romberg scheme attempted to iterate through the discontinuity. This is a quick, crude, practical solution to the problem, and probably more

sophisticated schemes could be developed that would allow closer approach of the integral limits to the endpoint roots but still guarantee continuity.

The integration across the endpoint pole involves two adjacent segments that must be considered together. A pre-integration sorting scheme identifies each segment as one of the following types:

Type 1 - Clean segment, no poles
Type 2 - Pole internal to endpoints
Type 3 - Pole at upper integration limit endpoint (lower wa-value)
Type 4 - Pole at lower integration limit endpoint (higher wa-value)

The integral across the pole is considered in the Cauchy principle value sense[12], which makes the basic assumption that the integral exists. We know that the Q(v) factor in the integrand is continuous, so that the only problem arises from the $1/(\zeta a - wa)$ singularity.

As an illustration of the application of the Cauchy principle value theorem to the integration across a pole, consider the simpler form

$$I = \int_1^5 \frac{dx}{x-2} \tag{4-4}$$

This can be computed as

$$I = \lim_{\varepsilon \to 0}\left[\int_1^{2-\varepsilon} \frac{dx}{x-2} + \int_{2+\varepsilon}^5 \frac{dx}{x-2}\right] = \lim_{\varepsilon \to 0}\left\{\left[\ln|x-2|\right]_1^{2-\varepsilon} + \left[\ln|x-2|\right]_{2+\varepsilon}^5\right\} = \lim_{\varepsilon \to 0}\left[\ln|-\varepsilon| - \ln|-1| + \ln|3| - \ln|\varepsilon|\right] \tag{4-5}$$

The terms in ε can be cancelled before taking the limit, giving, simply

$$I = \int_1^5 \frac{dx}{x-2} = \ln 3 = 1.10 \tag{4-6}$$

In the M-integral, the function Q(v) in the integrand prevents integration across the pole in closed form, so that an approximate method must be used. Consider the integration across the pole between arbitrary limits $\pm\varepsilon$ on either side of the pole, as shown in Figure 7. The integral is written as

$$SG = \int_{\zeta a+\varepsilon}^{\zeta a-\varepsilon} \frac{Q(v)}{\zeta a - wa} d(wa) \tag{4-7}$$

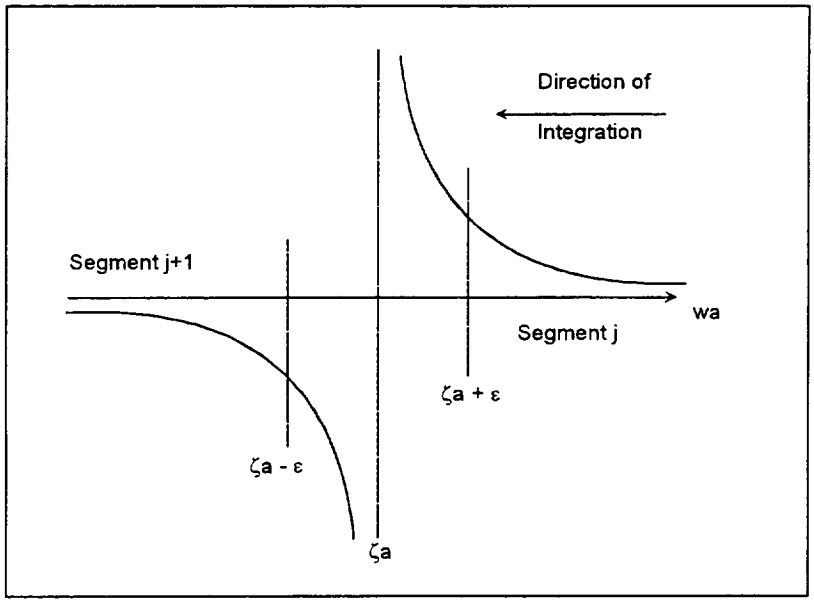

Figure 7. Integration across singularity on real axis

If ε is chosen sufficiently small, we can approximate Q(v) by a linear function, as illustrated in Figure 8 and written as

$$Q(x) = D_1 wa + D_0 \tag{4-8}$$

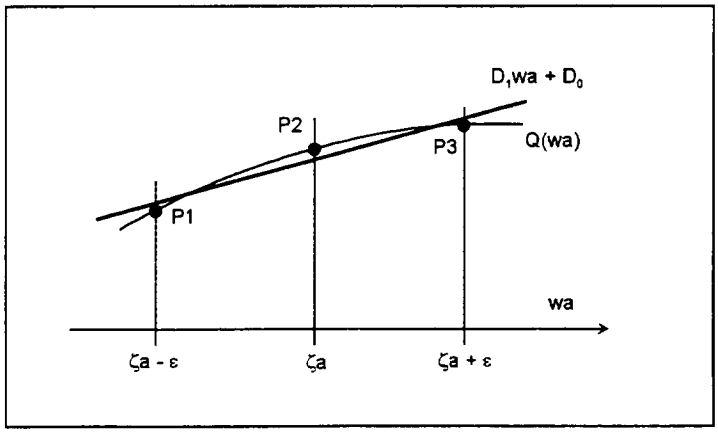

Figure 8. Linear fit to Q-function around pole

Then we can write

$$SG = -\int_{\zeta a+\varepsilon}^{\zeta a-\varepsilon} \frac{D_1 wa + D_0}{wa - \zeta a} d(wa) = -\left[\int_{\zeta a+\varepsilon}^{\zeta a-\varepsilon} \frac{D_1 wa}{wa - \zeta a} d(wa) + \int_{\zeta a+\varepsilon}^{\zeta a-\varepsilon} \frac{D_0}{wa - \zeta a} d(wa)\right] \tag{4-9}$$

When carried out in the principle value sense, this can be shown to give simply

$$SG = 2D_1\varepsilon \tag{4-10}$$

In the computer program, this contribution from the integral around the pole is added to the numerical integration for segment j taken up to $\zeta a + \varepsilon$, and the numerical integration for segment j+1 includes only the contribution from the integral starting at $\zeta a - \varepsilon$.

The coefficients D_0 and D_1 are obtained from a simple 3-point linear regression curve fit to the values of Q(v) at the points

P1: $wa_1 = \zeta a - \varepsilon$
P2: $wa_2 = \zeta a$
P3: $wa_3 = \zeta a \ \varepsilon$

as shown in Figure 8. An example of the accuracy of the linear assumption using $\varepsilon = 0.05$ is shown in Figure 9.

Examination of a few cases has indicated that $\varepsilon = 0.05$ is a reasonable assumption, introducing only small errors in the overall integral. The trade-off is in computation time, since the Romberg numerical integration scheme requires many more iterations to converge to the specified tolerance the closer the endpoint comes to (i.e., starts going up) the pole. A diagnostic program is available to examine the details of the variable-Ω integration along the real axis.

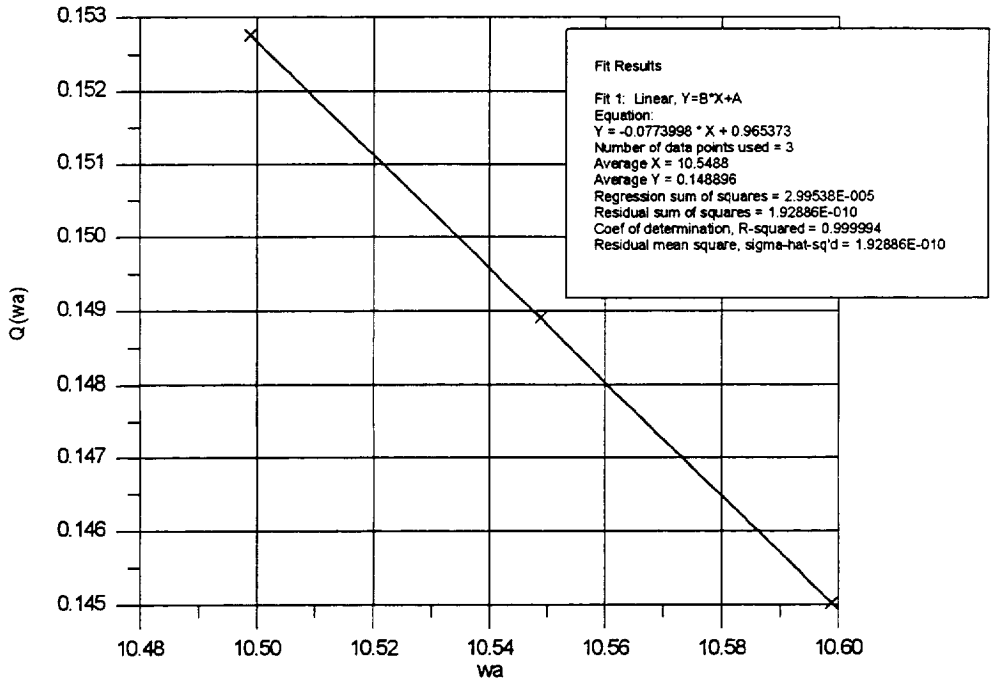

Figure 9. Linear fit of function Q(wa) around pole for m = 2, ζa = 10.54883, ka = 12.5, with $\varepsilon = 0.05$.

4.2 Real Axis, Constant Ω

The integral along the real axis with the constant-Ω numerator in the integrand can be written

$$GMCR(m) = \int_{k_{n,m-1}a}^{k_{nm}a} \frac{\Omega(v_{n,m-1})}{(\zeta a)^2 - (wa)^2} d(wa) \tag{4-11}$$

where Equation (4-2) still applies and there is an integral analogous to Equation (4-3) over the partial segment from $k_{n,m0}a$ to zero. The integral for GMCR can be computed in closed form, with special attention to integrating across any singularities.

Part of this integral, it will turn out, is required in a special form to be used to resolve an indeterminate in the reflection coefficient K_+ function. The form needed for this integral is solved by LHR (Reference 4, p. 48, Eqn (A-37)), and is given as

$$GMCR(m) = \sum_{m=1}^{m_0} \ln\left[\frac{k_{nm}a + \zeta a}{k_{nm}a - \zeta a}\right] + i\left[\Omega\left(v_{n,m_0}\right) + \Omega\left(v_{n,m_1}\right)\right] \tag{4-12}$$

where m_1 is the mode whose axial wavenumber is just greater than or equal to ζa. This integral includes the $2\zeta a/\pi$ multiplication factor that is not yet included in the other integrals.

To derive the integral in this form, LHR multiply the integrand in Equation (4-11) by $2\zeta a$ and expand as the sum

$$\frac{2\zeta a}{\zeta a^2 - wa^2} = \frac{1}{\zeta a + wa} + \frac{1}{\zeta a - wa} \tag{4-13}$$

They then operate on each of the resulting two integrals separately, solving each in closed form to give GMCR.

The summation of natural log term, when substituted into the exponential in $M(\zeta a)$, (see Equation (2-4)), becomes the factor

$$\exp\left(\sum_{m=1}^{m_0} \ln\left[\frac{k_{nm}a + \zeta a}{k_{nm}a - \zeta a}\right]\right) = \prod_{m=1}^{m_0}\left[\frac{k_{nm}a + \zeta a}{k_{nm}a - \zeta a}\right]^{\frac{1}{2}} \tag{4-14}$$

One of the factors in this multiple product will be combined with the $\sqrt{J_n'}$ factor in the reflection coefficient to resolve an indeterminate form. The remaining two constant terms are purely imaginary, and will affect only the phase of the reflection coefficient when substituted into the M-integral exponential.

4.3 Imaginary Axis, Variable Ω

For the integration over modes up the imaginary axis, we make the transformation of variable

$$wa = iy \tag{4-15}$$

so that y is a real variable of integration. Inserting this into the integral for each modal segment gives

$$GMVI(j) = i\int_{\kappa_{n,j-1}a}^{\kappa_{n,j}a} \frac{\Omega(v(y))}{\zeta a^2 + y^2}\,dy \tag{4-16}$$

where index j implies a cutoff mode order greater than m_0 and

$$i\kappa_{nj}a = k_{nj}a = i\sqrt{\gamma_{nj}^2 - (ka)^2} \tag{4-17}$$

making κ_{nj} real, since, for cutoff modes, $\gamma_{nj} > ka$.

The first value of j in Equation (4-16) will be $j = m_0+2$, that is, the second mode order above cutoff. We must also include the partial segment integral starting from $y = 0$,

$$GMVI(m_0+1) = i \int_0^{\kappa_{n,m0+1}a} \frac{\Omega(v(y))}{\zeta a^2 + y^2} dy \qquad (4\text{-}18)$$

In the sum of integrals over all real and imaginary mode segments, GMVR(m_0+1) from Equation (4-3) combines with GMVI(m_0+1) to give the total contribution of mode m_0+1 to the M-integral.

When transformed to the y-variable, the argument of the Bessel function in $\Omega(v)$ becomes

$$v(wa) = v(y) = \sqrt{(ka)^2 - (iy)^2} = \sqrt{(ka)^2 + y^2} \qquad (4\text{-}19)$$

which is real. Thus, the entire integrand of Equation (4-16) is real, and GMVI(j) is purely imaginary. This indicates that integral up the imaginary axis contributes only to the phase of the reflection coefficient, through the M-integral exponential.

It is assumed without proof that the sum of integrals up the imaginary axis converges to a finite value, and that only a finite number of terms need be included to obtain sufficient accuracy. This assumption will be examined later in test case computations.

Since $\Omega(v)$ is variable, the integration in Equations (4-16) and (4-18) must be computed numerically. This is accomplished using the Romberg method, which can be carried out as a real integral. All integrals are of the "clean segment" type, with no singularities, since ζa is real.

If it were desired to compute the reflection coefficient for a cut-off mode, such that ζa became imaginary, a method similar to the method of integration through a singularity on the real axis would have to be used on the imaginary axis. To reiterate, although reflection coefficients for scattering into or among cut-off modes are not calculated, the effect of the scattering into cutoff modes on the reflection coefficient of the cut-on modes (a phase shift effect) is included.

4.4 Imaginary Axis, Constant Ω

This integral, for each mode segment, can be written

$$GMCI(j) = i \int_{\kappa_{n,j-1}a}^{\kappa_{n,j}a} \frac{\Omega(v_{n,j-1})}{\zeta a^2 + y^2} dy \tag{4-20}$$

where the transformation of Equation (4-15) has been used to make the integral itself real. As in the case of GMVI, the integral over the partial segment from y = 0 to y = $\kappa_{n,m0+1}a$ must also be included.

There are no singularities in this integral, and, since the numerator is a constant over the mode segment, it can be evaluated in closed form as

$$GMCI(j) = i \frac{\Omega(v_{n,j-1})}{\zeta a} \left[\arctan\left(\frac{\kappa_{nj}a}{\zeta a}\right) - \arctan\left(\frac{\kappa_{n,j-1}a}{\zeta a}\right) \right] \tag{4-21}$$

LHR integrate this part using the same expansion of the denominator into two terms that they used to find GMCR, leading to a log sum solution. The form in Equation (4-21) is equivalent to the LHR form, and should be slightly easier to compute. No problem should be encountered by taking the principle value of the arctan function in Equation (4-21).

4.5 Final Form of the M-Integral

After shifting the multiple product factor in GMCR from the exponential of the M-integral to the multiplier of the exponential, the remainder of the M-integral can be written as

$$\begin{aligned} M(\zeta a) = {} & \frac{2\zeta a}{\pi} \left\{ \sum_{m=1}^{m_0} GMVR(m) + GMVR(m_0 + 1) \right\} - i\left[\Omega(v_{n,m_0}) + \Omega(v_{n,m_1})\right] \\ & + \frac{2\zeta a}{\pi} \left\{ \sum_{j=m_0+2}^{Max} GMVI(j) + GMVI(m_0 + 1) \right\} \\ & - \frac{2\zeta a}{\pi} \left\{ \sum_{j=m_0+2}^{Max} GMCI(j) + GMCI(m_0 + 1) \right\} \end{aligned} \tag{4-22}$$

where expressions for the integrals are derived above. Integrals that contain a "V" in the name must be evaluated numerically, while integrals with names containing a "C" are given by closed form expressions. The required procedures for integrating across singularities must be observed for computing the GMVR integrals. The sums of integrals up the imaginary axis are continued to some maximum value Max, and this must be suitably high to provide an acceptable convergence tolerance.

5. Computation of Reflection Coefficient

5.1 Final Computational Form

When the multiple product derived from the M-integral integration of the constant-Ω part of the integration along the real axis is combined with the $K_+(\zeta a)$ function from Equation (2-4), we obtain a new form:

$$K_+(\zeta a) = \sqrt{\pi(ka-\zeta a)\,J_n'(v)\,H_n'^{(1)}(v)}\sqrt{\prod_{m=1}^{m_o}\left[\frac{k_{nm}a+\zeta a}{k_{nm}a-\zeta a}\right]}\,e^{\frac{1}{2}M(\zeta a)} \tag{5-1}$$

where now $M(\zeta a)$ is the revised form given by Equation (4-22). Combining the radicals and rearranging slightly gives the square-root factor

$$RKF(\zeta a) = \sqrt{\pi(ka-\zeta a)\frac{J_n'(v)}{k_{nj}a-\zeta a}H_n'^{(1)}(v)(k_{nj}+\zeta a)\prod_{\substack{m=1\\ m\neq j}}^{m_o}\left[\frac{k_{nm}a+\zeta a}{k_{nm}a-\zeta a}\right]} \tag{5-2}$$

where the j^{th} factor in the multiple product has been extracted and its denominator associated with $J_n'(v)$.

As $\zeta a \Rightarrow k_{nj}a$, this ratio becomes an indeterminate form (0/0), since $v_{nj} = \gamma_{nj}$ is a root of the Bessel function derivative. Using L'Hospital's procedure for indeterminate forms (taking the derivative of the numerator and the denominator with respect to ζa before taking the limit), we can show that

$$\lim_{\zeta a\to k_{nj}a}\left[\frac{J_n'(v(\zeta a))}{k_{nj}a-\zeta a}\right] = \frac{k_{nj}a}{\gamma_{nj}^3}\left(n-\gamma_{nj}^2\right)J_n(\gamma_{nj}) \tag{5-3}$$

Since $J_n'(\gamma_{nl}) = 0$, we have

$$H_n'(\gamma_{nj}) = i\,Y_n'(\gamma_{nj}) \tag{5-4}$$

Using the Bessel function identity

$$J_n(x)Y_n'(x) - J_n'(x)Y_n(x) = \frac{2}{\pi x} \tag{5-5}$$

we have

$$i\,J_n(\gamma_{nj})Y_n'(\gamma_{nj}) = \frac{2i}{\pi\gamma_{nj}} \tag{5-6}$$

Using Equations (5-2) through (5-6), the product of the K_+ functions can finally be written as

$$K_+(k_{nm}a)K_+(k_{n\mu}a) = \frac{4ik_{n\mu}a\,k_{nm}a}{\gamma_{n\mu}^2\,\gamma_{nm}^2}\sqrt{(ka-k_{n\mu}a)(ka-k_{nm}a)(n^2-\gamma_{n\mu}^2)(n^2-\gamma_{nm}^2)\Pi_\mu\Pi_m} \tag{5-7}$$

where

$$\Pi_m = \prod_{\substack{j=1\\ j\neq m}}^{m_0}\left[\frac{k_{nj}a+\zeta a}{k_{nj}a-\zeta a}\right] \tag{5-8}$$

and

$$\Pi_\mu = \prod_{\substack{j=1\\ j\neq \mu}}^{m_0}\left[\frac{k_{nj}a+\zeta a}{k_{nj}a-\zeta a}\right] \tag{5-9}$$

This gives the final computational form for the reflection coefficient for the m^{th} radial mode reflecting into the μ^{th} radial mode:

$$R_{nm\mu} = -\frac{2k_{nm}}{\gamma_{nm}^2(k_{nm}a+k_{n\mu}a)}\frac{J_n(\gamma_{nm}a)}{J_n(\gamma_{n\mu}a)} \times\sqrt{\left((ka)^2-(k_{n\mu}a)^2\right)\left((ka)^2-(k_{nm}a)^2\right)\frac{n^2-\gamma_{nm}^2}{n^2-\gamma_{n\mu}^2}\Pi_\mu\Pi_m}\;e^{\frac{1}{2}M(k_{n\mu}a)} \tag{5-10}$$

where $M(k_{n\mu}a)$ is obtained from Equation (4-22).

5.2 Sample Calculations

An edited computer printout follows of the computation of the reflection coefficient for a test case, denoted Case #1, with n = 2, ka = 12.5, and $\varepsilon = 0.05$, where ε is the distance around the singularity used for the linear fit. Diagnostic results for the intermediate computations of the integrals are included in the Case #1 printout.

Note that for this value of ka, no modes are near cut-off, so that all reflection coefficient magnitudes are small, the largest being the R_{13} cross-term with a magnitude of 0.132. Note that from the results of the imaginary axis integrations that the last term for the 10th cut-off mode is about 3-5% of the sum for the constant-Ω or variable-Ω parts.

```
            PROGRAM CDRC1    TEST CASE #1

    CALCULATES MODAL REFLECTION COEFFICIENTS
    USING HOMICZ & LORDI M-INTEGRAL FORM

    SPINNING MODE ORDER M =    2
    ka =      12.50000000
    NUMBER OF CUT-ON MODES =     3
    NUMBER OF MODES IN CALC =    13
    EPSILON ABOUT POLE =       .050000

    EIGENVALUES AND PROPAGATION CONSTANTS
    ROOTA ARE INTEGRATION SEGMENT ENDPOINTS

 MODE              EV         PKA REAL         PKA IMAG            ROOTA

    1       3.05423700      12.12112000        .00000000      12.12112000
    2       6.70613300      10.54883000        .00000000      10.54883000
    3       9.96946800       7.54053700        .00000000       7.54053700
    4      13.17037000       -.00000018      4.14833500         .00000000
    5      16.34752000       -.00000046     10.53525000       4.14833400
    6      19.51291000       -.00000065     14.98345000      10.53525000
    7      22.67158000       -.00000083     18.91430000      14.98345000
    8      25.82604000       -.00000099     22.59943000      18.91430000
    9      28.97767000       -.00000114     26.14298000      22.59943000
   10      32.12733000       -.00000129     29.59586000      26.14298000
   11      35.27554000       -.00000144     32.98656000      29.59586000
   12      38.42265000       -.00000159     36.33250000      32.98656000
   13      41.56894000       -.00000173     39.64501000      36.33250000
   14        .00000000        .00000000       .00000000      39.64500000

REAL AXIS INTEGRATIONS:
GV2 ARE SEGMENT INTEGRALS FOR VARIABLE OMEGA PART
JS = SEGMENT #:  ISX = OMEGA MULTIPLIER:  ITP = SEGMENT TYPE
FOMM0 AND FOMMZ ARE TERMS IN CONSTANT OMEGA INTEGRATION
JM = RADIAL MODE NUMBER: GMR = TOTAL REAL AXIS INTEGRAL

    JS ISX ITP             GV2
    1   0   3   -3.1993660E-02
    2   1   4   -1.4871500E-01
    3   2   1   -2.3233030E-01
    4   3   1   -4.7253740E-01

  JM=   1 FOMM0=   6.2832600E+00 FOMMZ=   2.5844570E-04

  REAL AXIS INTEGRAL, JM=  1 GMR=  -6.8335920E+00+  6.2835190E+00*i

    JS ISX ITP             GV2
    1   0   1   -2.2201310E-03
    2   1   3    3.7623970E-01
    3   2   4   -8.1834660E-01
    4   3   1   -6.6436000E-01

  JM=   2 FOMM0=   6.2832600E+00 FOMMZ=   3.1417410E+00
```

REAL AXIS INTEGRAL, JM= 2 GMR= -7.4454900E+00+ 9.4250010E+00*i

JS	ISX	ITP	GV2
1	0	1	-9.2672090E-04
2	1	1	4.1502940E-02
3	2	3	1.4690930E+00
4	3	4	-2.7157840E+00

JM= 3 FOMM0= 6.2832600E+00 FOMMZ= 6.2832600E+00

REAL AXIS INTEGRAL, JM= 3 GMR= -5.7899020E+00+ 1.2566520E+01*i

IMAGINARY AXIS INTEGRALS FOR 10 CUTOFF MODES
X1 & X2 ARE SEGMENT ENDPOINTS ON IMAGINARY AXIS
GCI IS CONSTANT OMEGA PART; GVI = VARIABLE OMEGA PART
NOTE THAT GCI AND GVI ARE IMAGINARY NUMBERS

JS	ISX	X1	X2	GCI	GVI	NST
1	3	.0000000	4.1483340	2.3842440E-01	2.4418080E-01	2
2	4	4.1483340	10.5352500	2.9995660E-01	3.4049100E-01	2
3	5	10.5352500	14.9834500	1.8152870E-01	2.0208300E-01	1
4	6	14.9834500	18.9143000	1.4290520E-01	1.5618500E-01	1
5	7	18.9143000	22.5994300	1.2069470E-01	1.3015610E-01	1
6	8	22.5994300	26.1429800	1.0551070E-01	1.1265110E-01	1
7	9	26.1429800	29.5958600	9.4195800E-02	9.9799390E-02	1
8	10	29.5958600	32.9865600	8.5317340E-02	8.9842860E-02	1
9	11	32.9865600	36.3325000	7.8105830E-02	8.1842490E-02	1
10	12	36.3325000	39.6450000	7.2101210E-02	7.5241620E-02	1

INTEGRAL TOTALS (JM,GVI,GCI,GMISUM)
1 1.5324740E+00 1.4187410E+00 2.2773180E+01

M-INTEGRAL FOR MODE JM= 1
GM= -6.8335920E+00 + 2.9056700E+01*i

JS	ISX	X1	X2	GCI	GVI	NST
1	3	.0000000	4.1483340	3.1129010E-01	3.1873770E-01	2
2	4	4.1483340	10.5352500	3.6638410E-01	4.1483920E-01	1
3	5	10.5352500	14.9834500	2.0563030E-01	2.2870910E-01	1
4	6	14.9834500	18.9143000	1.5587390E-01	1.7028760E-01	1
5	7	18.9143000	22.5994300	1.2871610E-01	1.3877520E-01	1
6	8	22.5994300	26.1429800	1.1088770E-01	1.1837650E-01	1
7	9	26.1429800	29.5958600	9.8001730E-02	1.0382320E-01	1
8	10	29.5958600	32.9865600	8.8121140E-02	9.2790350E-02	1
9	11	32.9865600	36.3325000	8.0236280E-02	8.4071740E-02	1
10	12	36.3325000	39.6450000	7.3760720E-02	7.6971370E-02	1

INTEGRAL TOTALS (JM,GVI,GCI,GMISUM)
2 1.7473820E+00 1.6189020E+00 2.2606590E+01

M-INTEGRAL FOR MODE JM= 2
GM= -7.4454900E+00 + 3.2031590E+01*i

JS	ISX	X1	X2	GCI	GVI	NST
1	3	.0000000	4.1483340	5.8457050E-01	5.9809270E-01	2
2	4	4.1483340	10.5352500	5.5824050E-01	6.2806500E-01	2
3	5	10.5352500	14.9834500	2.5824970E-01	2.8668140E-01	2
4	6	14.9834500	18.9143000	1.8100920E-01	1.9758640E-01	2
5	7	18.9143000	22.5994300	1.4326990E-01	1.5440400E-01	1
6	8	22.5994300	26.1429800	1.2024990E-01	1.2834160E-01	1
7	9	26.1429800	29.5958600	1.0444730E-01	1.1063630E-01	1
8	10	29.5958600	32.9865600	9.2777270E-02	9.7684410E-02	1
9	11	32.9865600	36.3325000	8.3723440E-02	8.7720260E-02	1
10	12	36.3325000	39.6450000	7.6447380E-02	7.9771590E-02	1

INTEGRAL TOTALS (JM,GVI,GCI,GMISUM)
3 2.3689840E+00 2.2029860E+00 2.1947530E+01

```
M-INTEGRAL FOR MODE JM=   3
GM=  -5.7899020E+00 +   3.4514050E+01*i
```

REFLECTION COEFFICIENTS - PHASE IN DEGREES

JM	JL	REAL-RC	IMAG-RC	RCMAG	RCPHS
1	1	4.7273920E-02	4.6988270E-02	6.6653740E-02	44.8264
1	2	5.8429380E-02	4.9116320E-02	7.6330890E-02	40.0507
1	3	-1.2287330E-01	-4.7580420E-02	1.3176390E-01	-158.8320
2	1	3.3685690E-02	2.8316530E-02	4.4006270E-02	40.0507
2	2	-4.1341060E-02	-2.9244140E-02	5.0638940E-02	-144.7249
2	3	-8.4828000E-02	-2.4953930E-02	8.8422210E-02	-163.6076
3	1	-3.5215500E-02	-1.3636560E-02	3.7763570E-02	-158.8320
3	2	-4.2169790E-02	-1.2405130E-02	4.3956550E-02	-163.6076
3	3	7.8862390E-02	-3.4299810E-03	7.8936950E-02	-2.4904

Case #2 below is the same as Case #1 except that ε is reduced to 0.02. Comparing the reflection coefficients for this case with Case #1 indicates very small differences in the reflection coefficient magnitudes and no difference in the phases. This indicates that, at least for n = 2, ε = 0.05 is a reasonably good assumption, and the total reflection coefficient computation at ε = 0.05 takes only a few seconds on a 33MHz IBM-PC 486.

```
            PROGRAM CDRC1   TEST CASE 2

    CALCULATES MODAL REFLECTION COEFFICIENTS
    USING HOMICZ & LORDI M-INTEGRAL FORM

    SPINNING MODE ORDER M =   2
    ka =     12.50000000
    NUMBER OF CUT-ON MODES =    3
    NUMBER OF MODES IN CALC =   13
    EPSILON ABOUT POLE =      .020000
```

EIGENVALUES AND PROPAGATION CONSTANTS

MODE	EV	PKARL	PKAIM	ROOTA
1	3.05423700	12.12112000	.00000000	12.12112000
2	6.70613300	10.54883000	.00000000	10.54883000
3	9.96946800	7.54053700	.00000000	7.54053700
4	13.17037000	-.00000018	4.14833500	.00000000
5	16.34752000	-.00000046	10.53525000	4.14833400
6	19.51291000	-.00000065	14.98345000	10.53525000
7	22.67158000	-.00000083	18.91430000	14.98345000
8	25.82604000	-.00000099	22.59943000	18.91430000
9	28.97767000	-.00000114	26.14298000	22.59943000
10	32.12733000	-.00000129	29.59586000	26.14298000
11	35.27554000	-.00000144	32.98656000	29.59586000
12	38.42265000	-.00000159	36.33250000	32.98656000
13	41.56894000	-.00000173	39.64501000	36.33250000
14	.00000000	.00000000	.00000000	39.64500000

REFLECTION COEFFICIENTS

JM	JL	RL-RC	IM-RC	RCMAG	RCPHS
1	1	4.7286910E-02	4.7001180E-02	6.6672050E-02	44.8264
1	2	5.8450030E-02	4.9133670E-02	7.6357860E-02	40.0507
1	3	-1.2288450E-01	-4.7584760E-02	1.3177600E-01	-158.8320
2	1	3.3697590E-02	2.8326530E-02	4.4021820E-02	40.0507
2	2	-4.1358900E-02	-2.9256770E-02	5.0660800E-02	-144.7249
2	3	-8.4842400E-02	-2.4958170E-02	8.8437220E-02	-163.6076
3	1	-3.5218710E-02	-1.3637800E-02	3.7767010E-02	-158.8320
3	2	-4.2176950E-02	-1.2407230E-02	4.3964010E-02	-163.6076
3	3	7.8855130E-02	-3.4296650E-03	7.8929690E-02	-2.4904

The reflection coefficient $R_{JM,JL}$ is the factor by which the JM^{th} forward-travelling radial mode is multiplied to give the contribution of the JM forward mode to the backward-travelling JL mode. The magnitude of the complex value $R_{JM,JL}$ gives the factor by which the amplitude of the component of the reflected mode decreases, and the phase of $R_{JM,JL}$ is gives the phase shift of the reflected mode component.

Figure 10 shows the computation of the R_{33} reflection coefficient magnitude and phase as a function of ka for frequencies just above cut-off of the n = 2, j = 3 mode to a ka value just below cut-on for the j = 4 mode. The reflection coefficient appears to be tending toward a value of 1.0 in magnitude and -180° in phase at the cut-off ka-value. As ka approaches the cut-off ka, the value of ε must be decreased to keep it between ka and the cut-off point.

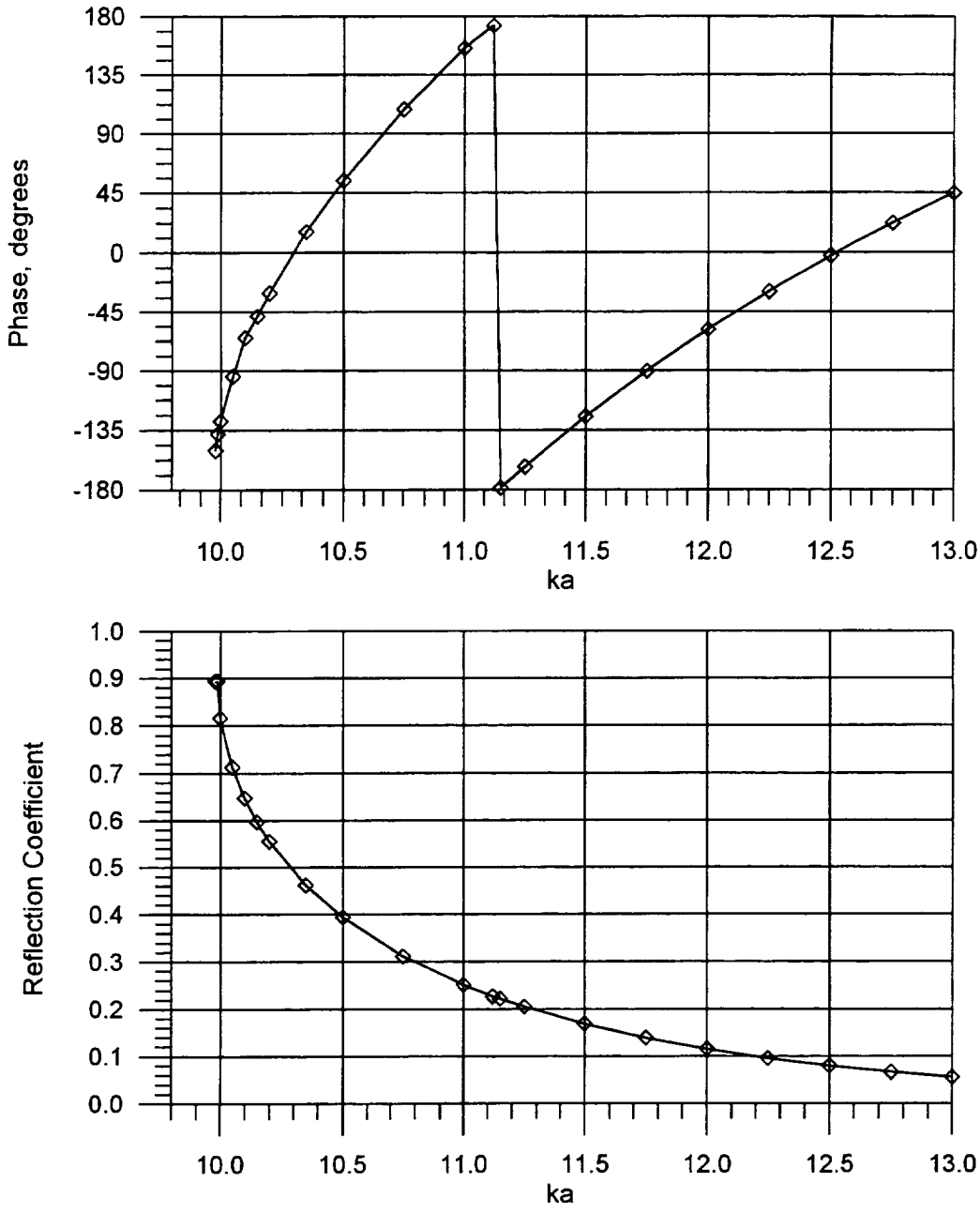

Figure 10. Magnitude and phase of reflection coefficient for R33, m = 2 (cutoff at ka = 9.97).

6. Conclusions and Recommendations

A computational method to predict modal reflection coefficients in cylindrical ducts has been developed and gives reasonable results. Reliable data to use for comparison is scarce, so complete checkout is difficult. Further checkout is needed over a wider range of system parameters. One suggestion is to compare the computations versus a finite element prediction model.

The method will be adapted as a subroutine to the GEAE segmented cylindrical duct modal analysis.

A near-term extension would be to apply the analysis to the prediction of the complex farfield directivity pattern, which can be done directly. The M-integral in the farfield case should be the same, only the algebraic factor is different. There may be other indeterminate forms to be resolved.

Upgrades that should be considered are to include the effect of mean flow in the duct and to examine the difficulty of extending the analysis to annular ducts.

The computation could be improved by adjusting the starting value of the integration along the real axis based on the behavior of the Ω-function for wa near ka. In this case, Y'_n goes to infinity but Ω goes to zero. Currently, the arbitrary value of $wa = ka - 0.05$ is used, but a better method to determine the starting value has been developed that could be incorporated into the numerical integration subroutine.

The analysis could be upgraded to double precision, particularly the determination of the Bessel function roots, but there is probably more error in the integral approximations and the assumption of an idealized unflanged pipe than this would warrant. Numerical precisions in the computation are currently fairly well "balanced".

The method could be extended to include a variable number of cut-off modes in the integral up the imaginary axis, so that convergence properties could be examined. The computation could also easily be extended to predict the reflection coefficient for cut-off modes.

7. References

[1] Kraft, R. E., and Kontos, K. B., "Theoretical Implications of Active Noise Control for Turbofan Engines", AIAA 93-4355, October, 1993.

[2] Rice, E. J., "Propagation of Waves in an Acoustically Lined Duct with a Mean Flow", NASA SP-207, July, 1969, pp. 345-355.

[3] Zorumski, W. E., "Generalized Radiation Impedances and Reflection Coefficients of Circular and Annular Ducts", J. Acoustical Soc. Amer, V54, No. 6, 1973, pp. 1667-1673.

[4] Lordi, J. A., Homicz, G. F., and Rehm, R. G., "Effects of Finite Duct Length and Blade Chord on Noise Generation by a Rotating Blade Row", AIAA 74-555, April, 1974.

[5] Lordi, J. A., Homicz, G. F., and Rehm, R. G., "Theoretical Studies on Fan Noise Generation by a Transonic Compressor Blade Row", Calspan Corporation, Report No. AI-2836-A-2, August, 1973.

[6] Noble, B., *Methods Based on the Wiener-Hopf Technique*, Pergamon Press, 1958.

[7] Levine, H. and Schwinger, J., "On the Radiation of Sound from an Unflanged Circular Pipe", Phys. Rev., 73, 1948, pp. 383+.

[8] Weinstein, L. A., *Theory of Diffraction and the Factorization Method (Generalized Wiener-Hopf Technique)*, Golem Press, 1969.

[9] Crighton, D. G., Dowling, A. P., Ffowcs Williams, J. E., Heckl, M., and Leppington, F. G., *Modern Methods in Analytical Acoustics: Lecture Notes*, Springer-Verlag, 1992 (Chapter 5.).

[10] Lordi, J. A., Homicz, G. F., and Rehm, R. G., "Theoretical Studies on Fan Noise Generation by a Transonic Compressor Blade Row", Calspan Corporation, Report No. AI-2836-A-2, August, 1973, p. 44.

[11] Press, W. H., Teukolsky, S. A., Vetterling, W. T., and Flannery, B. P., *Numerical Recipes in FORTRAN: The Art of Scientific Computing*, Cambridge University Press, 1992, p. 134ff.

[12] Jeffrey, A., *Complex Analysis and Applications*, CRC Press, 1992, p. 382.

REPORT DOCUMENTATION PAGE

Form Approved
OMB No. 0704-0188

1. AGENCY USE ONLY (*Leave blank*)	2. REPORT DATE	3. REPORT TYPE AND DATES COVERED
	September 1996	Final Contractor Report

4. TITLE AND SUBTITLE

Active Control of Fan Noise: Feasibility Study
Volume 5: Numerical Computation of Acoustic Mode Reflection Coefficients for an Unflanged Cylindrical Duct

5. FUNDING NUMBERS

WU-538-03-11
C-NAS3-26617

6. AUTHOR(S)

R.E. Kraft

7. PERFORMING ORGANIZATION NAME(S) AND ADDRESS(ES)

General Electric Aircraft Engines
1 Neumann Way
P.O. Box 156301
Cincinnati, Ohio 45214-6301

8. PERFORMING ORGANIZATION REPORT NUMBER

E-10379

9. SPONSORING/MONITORING AGENCY NAME(S) AND ADDRESS(ES)

National Aeronautics and Space Administration
Lewis Research Center
Cleveland, Ohio 44135-3191

10. SPONSORING/MONITORING AGENCY REPORT NUMBER

NASA CR-198513

11. SUPPLEMENTARY NOTES

Project Manager, Laurence J. Heidelberg, Propulsion Systems Division, NASA Lewis Research Center, organization code 2770, (216) 433-3859.

12a. DISTRIBUTION/AVAILABILITY STATEMENT

Unclassified - Unlimited
Subject Categories 07 and 71

This publication is available from the NASA Center for AeroSpace Information, (301) 621-0390.

12b. DISTRIBUTION CODE

13. ABSTRACT (*Maximum 200 words*)

A computational method to predict modal reflection coefficients in cylindrical ducts has been developed based on the work of Homicz, Lordi, and Rehm, which uses the Wiener-Hopf method to account for the boundary conditions at the termination of a thin cylindrical pipe. The purpose of this study is to develop a computational routine to predict the reflection coefficients of higher order acoustic modes impinging on the unflanged termination of a cylindrical duct. This effort was conducted under Task Order 5 of the NASA Lewis LET Program, *Active Noise Control of Aircraft Engines: Feasibility Study*, and will be used as part of the development of an integrated source noise, acoustic propagation, ANC actuator coupling, and control system algorithm simulation. The reflection coefficient prediction will be incorporated into an existing cylindrical duct modal analysis to account for the reflection of modes from the duct termination. This will provide a more accurate, rapid computation design tool for evaluating the effect of reflected waves on active noise control systems mounted in the duct, as well as providing a tool for the design of acoustic treatment in inlet ducts. As an active noise control system design tool, the method can be used preliminary to more accurate but more numerically intensive acoustic propagation models such as finite element methods. The resulting computer program has been shown to give reasonable results, some examples of which are presented. Reliable data to use for comparison is scarce, so complete checkout is difficult, and further checkout is needed over a wider range of system parameters. In future efforts the method will be adapted as a subroutine to the GEAE segmented cylindrical duct modal analysis program.

14. SUBJECT TERMS

Acoustic ducts; Fan noise; Ducted fans

15. NUMBER OF PAGES

31

16. PRICE CODE

A03

17. SECURITY CLASSIFICATION OF REPORT	18. SECURITY CLASSIFICATION OF THIS PAGE	19. SECURITY CLASSIFICATION OF ABSTRACT	20. LIMITATION OF ABSTRACT
Unclassified	Unclassified	Unclassified	